SUPPLEMENTARY MATERIALS

1

Supplementary methods

Ethics statement

The maintenance and breeding of mouse lines and all experiments were approved by the Committee on Animal Health and Care of the local government body of the state of Upper Bavaria (Regierung von Oberbayern; TVA 55.2-1-54-2532-214-2013 and TVA 55.2-1-54-2532-217-2014) and performed in strict compliance with the EEC recommendations for the care and use of Lab. Anim. (European Communities Council Directive of 24 November 1986 (86/609/EEC)). The use of surgically resected CD patient samples was approved by AFFSAPS (IDRCB: 2009-A00205-52), the French Ethic Committee- Hôpital Saint-Louis (CPP 2009/17) and declared to clinicaltrials.gov (NCT03458195). All patients provided an informed written consent. For generation of human organoids, the use of surgically resected human tissue samples was approved by the Ethics Committee of the Medical Faculty of TUM and obtained after prior informed written consent.

Animals

$Hsp60^{flox/flox}$ mice and $Hsp60^{flox/flox}$ x $Lgr5$CreER^{T2}-IRES-$Egfp^{Tg}$ mice (to generate ISC-specific Hsp60 knockout mice via tamoxifen-induction ($Hsp60^{\Delta/\Delta ISC}$ mice) were generated as described previously [1]. TNF$^{\Delta ARE}$ mice were initially provided from Case Western University, Cleveland. All mice were housed (12h light/ dark cycles, 24-26°C) under SPF conditions and bred for several generations in the animal facility to harmonize the intestinal microbiota. Mice received a standard diet (autoclaved V1124-300; Ssniff, Soest, Germany) and autoclaved water ad libitum. Animals were killed by CO_2 inhalation. TNF$^{\Delta ARE}$ mice and WT littermates were sacrificed at 18 weeks of age.

Induction of postnatal recombination and monitoring of mice

Phytoestrogen free pellets (ssniff, Soest, Germany) were fed for 4 weeks to male 6 weeks old $Hsp60^{flox/flox}$ X $Lgr5CreER^{T2}$ $Egfp^{Tg}$ and their appropriate control mice, respectively. Afterwards, they received 400 mg tamoxifen citrate (Tam) per kg chow feed (LASvendi, Soest, Germany) in pellets *ad libitum* for 7 days. Body weight was monitored before, during and after oral administration of tamoxifen. Body weight, general condition, behavior and intestinal symptoms were assessed by a score

2

between 0 and 10 each according to the approved application for animal experiments. Animals were sacrificed at the indicated time points.

Mouse Tissue processing and histopathological analysis

The intestine was removed immediately after killing, trimmed free of adjacent tissue and cleaned of stool. Small intestinal tissues were either immediately fixed for preparation of cross sections or cut open and prepared as a 'swiss role'. Tissues were fixed in 4% PBS buffered formaldehyde, dehydrated and embedded in paraffin (FFPE). For histopathological assessment, 5 µm sections were stained with hematoxylin (of Mayer) and 0.2% eosin (ethanolic solution; both Medite, Burgdorf, Germany) in an automated staining machine (Leica, Soest, Germany). Ileal sections were blindly assessed for mononuclear cell infiltration into lamina propria, crypt hyperplasia, goblet cell depletion and ulcer formation resulting in a score from 0 (not inflamed) to 12 (highly inflamed) as described previously [4].

Transmission electron microscopy (TEM)

For TEM analysis, longitudinal sections of freshly dissected ileum samples were fixed in 2.5% electron microscopy grade glutaraldehyde in 0.1 M sodium cacodylate buffer pH 7.4 (Science Services, Munich, Germany), postfixed in 2% aqueous osmium tetraoxide (Dalton, 1955), dehydrated in gradual ethanol (30–100%) and propylene oxide, embedded in Epon (Merck, Darmstadt, Germany) and cured for 24 hours at 60°C. Semithin sections were cut and stained with toluidine blue. Ultrathin sections of 50 nm were mounted on 200 mesh copper grids, contrasted with uranyl acetate and lead citrate before examination by transmission electron microscopy (Zeiss Libra 120 Plus, Carl Zeiss NTS GmbH, Oberkochen, Germany). Pictures were acquired at 1260-12500x magnification, using a Slow Scan CCD-camera and iTEM software (Olympus Soft Imaging Solutions, Münster, Germany).

Samples from Crohn's disease patients

CD patients' tissue samples were collected during a prospective multicenter study performed by the REMIND group published previously [5]. From this cohort, 70 patients with a paraffin-embedded ileal margin sample available for histological analysis were selected [6]. Patients' characteristics at time of surgery are given in **Supplementary table 1**. Briefly, to assess inflammation at time of surgery, full-thickness 3-µm sections

3

of paraffin-embedded ileal margin were stained with hematein eosin saffron (HES). Each section was jointly analyzed by two expert pathologists blinded to the baseline detailed clinical data and to the post-operative outcomes of the patients. The ileal margin was considered as inflamed if (i) mucosal erosion or ulceration or (ii) cryptic abscess/cryptitis was noticed. Ileocolonoscopy was performed 6 -12 months after surgery. The physician performing the endoscopy evaluated the Rutgeerts score. Two physicians checked the colonoscopy's report blinded to histological analysis and post-operative treatment. Endoscopic recurrence was defined as a Rutgeerts score ≥ i2.

Staining procedures

Immunohistochemical (IHC) and immunofluorescence (IF) stainings were performed on 4 µm FFPE tissue sections as described previously [1]. To stain intestinal organoids, Matrigel containing organoids was gently dissolved in cold PBS (Sigma-Aldrich, Taufkirchen, Germany), centrifuged for 5 min at 300 g, and pelleted organoids were carefully fixed in 4% formaldehyde. The suspension was transferred to a microscope glass slide, incubated for 15 min at room temperature and washed subsequently before starting the described [1] staining procedure by adding blocking buffer. Antibodies and dilutions are given in **Supplementary Table 2 and 3**. For detection of apoptosis in FFPE tissue sections (TUNEL-assay) the Apo-BrdU *In Situ* Fragmentation Assay Kit (BioVision, Milpitas, CA) was used according to the manufacturer's instructions. Tissue sections treated with DNaseI (Macherey-Nagel, Düren, Germany) for 15 min immediately after antigen retrieval served as positive controls for the TUNEL assay, murine intestinal segments incubated *ex vivo* in 1 µM staurosporine for 2 h at 37 °C before embedding served as positive controls for CC3 staining. For IF, stainings were visualized using the Flouview FV10i microscope (Olympus, Shinjuku, Japan). For IHC co-staining, sections were incubated for 20 min with 3% H_2O_2 (Sigma- Aldrich, Taufkirchen, Germany) after the first antigen detection using the DAB enhanced liquid substrate system (Sigma-Aldrich). Subsequently, sections were blocked and a second antibody was applied as described above. To detect the second antigen, the HRP green solution set (42 Life sciences GmbH, Bremerhaven, Germany) was used. IHC stainings were scanned and further analyzed using a PreciPoint M8 microscope (Precipoint, Freising, Germany).

4

In situ hybridization

In situ hybridization for murine *Lgr5,* human *LGR5* and *Olfm4* was performed on 5µm thick tissue sections using the RNAscope-2.5 HD *in situ* assay kit-Brown (ACD, Bio-Techne GmbH, Wiesbaden, Germany) according the manufacturer's instructions. Probes were :RNAscope Probe-Mm-Lgr5; RNAscope Probe-Mm-*Olfm4*; RNAscope Probe-Mm-*Hopx,* and RNAscope Probe-Hs-*LGR5*, all from ACD. Sections were counterstained with hematoxylin, dipped in 0.02% ammonium hydroxide solution and were mounted with xylene based mounting medium. For IHC co-staining, tissue sections were incubated with 3% H_2O_2 (Sigma-Aldrich) for 20 min after conducting *in situ* hybridization stained as described above. For detection of IHC-stained antigens the HRP green solution set (42 Life sciences GmbH, Bremerhaven, Germany) was used. Sections were counterstained with hematoxylin and mounted with xylene based mounting medium. Stained slides were scanned and further analyzed via the PreciPoint M8 microscope.

Quantification of Lysozyme and Lgr5 positive cells

Numbers of Lysozyme (Lyz/LYZ) positive and *Lgr5/LGR5* positive cells were determined in ileal tissue sections stained for Lyz/LYZ by IF and for *Lgr5/LGR5* by *in situ* hybridization. A total number of 80 (for human) or 50 (for mice) well oriented crypts were quantified. Signals arising from cells below the +7 position (<+7) were considered to be located in lower crypt, upper crypt was defined as >+7 (**Supplemental Fig.4A**). To assess *Lgr5/LGR5* expression, dots representing *Lgr5/LGR5* transcripts were counted and crypts containing ≥15 transcripts (for human) and ≥10 transcripts (for mice), respectively, were considered as crypts with high *Lgr5* expression. To assess the granularity of Lyz/LYZ positive cells, a minimum of 150 PCs (ranges between 150 and 334 PCs) were quantified in human tissue sections, for mice all PCs contained in 50 crypts were analyzed. Lyz/LYZ positive cells were considered as highly granular if ≥2 Lyz/LYZ positive granules were visible within the cell. The quantification was performed in a blinded manner.

Quantification of Olfm4 and HopX expression

Quantification of *Olfm4* and *Hopx* expression was performed in small intestinal tissue sections stained by *in situ* hybridization. For TNF$^{\Delta ARE}$ mice, a total number of 50 well oriented ileal crypts were quantified. Total numbers of *Olfm4* positive cells were

5

determined in the crypt base (<+7 cells, Supplemental Fig. 4A). For $Hsp60^{\Delta/\Delta ISC}$ mice, images of *Hopx in situ* hybridization stainings were analyzed using the ImageJ software. In at least 30 open, well-oriented crypts total crypt IEC area up to the crypt-villus junction was defined and within this area, the area positive for the respective staining was determined. For *Olfm4*, owing to the discontinuous expression pattern of this marker gene, the distance of the most upper *Olfm4* positive cell to the crypt ground (position 0) was measured and normalized to crypt length. All quantifications were performed in a blinded manner.

Quantification of Hsp60 expression

Volocity 2D-3D imaging software was used for the quantification of fluorescence intensity in IF stained tissue section. Quantification of the Hsp60 signals was performed in a minimum of 30 well oriented intestinal crypts. The crypt base area was selected according to **Supplemental Fig. 4A** (<+7 cells) and the positive signal was quantified based on the best fitting threshold, covering positive areas of the crypt base. The same threshold was used for quantification of all sections.

Isolation of primary IECs

Primary IEC were purified as previously described [1]. Approximately 6 cm of intestine were inverted on a needle, vortexed vigorously and incubated (37 °C, 15 min) in DMEM containing 10% fetal calf serum (FCS superior, Biochrom, Berlin), 1.0% Glutamine, 0.8% antibiotics/antimycotics (all Sigma-Aldrich, St Louis, MO) supplemented with 1 mM dithiothreitol (Roth, Karlsruhe, Germany). The IEC suspensions were centrifuged (7 min, 300g, RT) and cell pellets were re-suspended in DMEM containing fetal calf serum, L-glutamine and antibiotics. The remaining tissue was incubated in 20 ml PBS (10 min, 37 °C) containing 1.5 mM EDTA (Roth). Thereafter, the tissue was discarded and the cell suspension from this step was centrifuged as mentioned above. Finally, primary IEC were purified by centrifugation through a 20%/40% discontinuous Percoll gradient (GE Healthcare, Uppsala, Sweden) at 600g for 30 min.

Primary crypt isolation and intestinal organoid culture

Primary small intestinal crypts from mouse (ileum, jejunum) and human (ileum) were isolated by tissue incubation in 2mM EDTA (Fisher, Dreieich, Germany) and cultured as described elsewhere [1, 7]. Briefly, crypts were embedded in 25µl matrigel (BD

Biosciences, Franklin Lakes, NJ) and cultured in 48 well plates. Until otherwise indicated, murine organoids were grown in crypt culture medium (CCM), advanced DMEM/F12 medium (Gibbco, Cincinnati, OH) containing 2 mM GlutaMax (Gibbco), 10 mM HEPES, penicillin, streptomycin and amphotericin (all Sigma- Aldrich, Taufkirchen, Germany) supplemented with N2, B27 (both Gibbco), 1 mM N-acetylcystein (Sigma- Aldrich), 50 ng ml−1 EGF (ImmunoTools, Friesoythe, Germany), 100 ng ml−1 noggin and 0.5 µg ml−1 R-spondin 1 (both PeproTec, Rocky Hill, NJ). Medium containing Wnt factors suitable for murine organoids (Intesticult) was obtained from STEMCELL Technologies, Grenoble, France. Human organoids were kindly provided by Tamara Zietek and maintained in Human Intesticult medium (STEMCELL Technologies, Grenoble, France). Two days prior to the start of experiments, medium of human organoids was changed to CCM. To assess seeding efficiency, total numbers of propagating organoids were counted at day 1 after seeding (baseline) and numbers of viable organoids were subsequently determined at the indicated time points in the same cell culture plate wells. Data are presented as proportion of living organoids over baseline counts. For quantification of *de novo* crypt formation (budding), organoids were classified according to number of visible bud structures (0, 1, 2, 3, >4). A minimum of 80 organoids (ranging between 80-140) was included in the analyses. *Ex vivo* induction of the *Hsp60* knockout was achieved by adding 1.5 µl of 100 µM (Z)-4-hydroxytamoxifen (4-OHT; LKT, St Paul, MN) to 300 µl CCM per well of a 48 well plate. When indicated, 2.5µM oligomycin (Sigma- Aldrich, Taufkirchen, Germany) or 15mM DCA (Sigma- Aldrich, Taufkirchen, Germany) were added to the culture medium for 24h. Growth measurements were performed using an Olympus CK X 41 microscope and Olympus cellSens Entry software.

Measurement of living cells and cellular ATP content

Life- and dead- cell protease activity was measured using the MultiTox-Fluor Cytotoxicity Assay and ATP content was measured using the CellTiter-Glo Luminescent Cell Viability Assay (both from Promega, Mannheim, Germany), according to the manufacturer's instructions in a 96-well format. Fluorescence and luminescence were measured using the Tecan infinite M200 (Tecan Group Ltd., Männedorf, Switzerland) and the i-control™ Microplate Reader software (Tecan, Grödig, Austria).

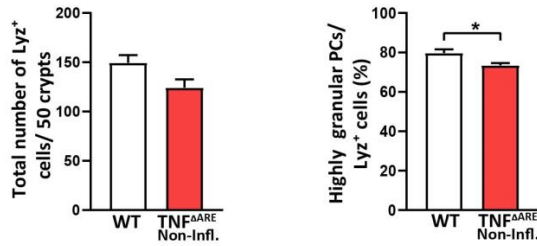### mRNA isolation and quantitative real-time PCR

RNA of a total ileal tissue, ileal IECs, primary crypts and small intestinal organoids was isolated using the NucleoSpin RNAII kit (Macherey-Nagel, Düren, Germany) according to the manufacturer's instructions. Quantitative Real-time PCR (qRT–PCR) was performed using 1 µl cDNA in a Light Cycler 480 system (Roche Diagnostics, Mannheim, Germany) applying the Universal Probe Library system according to the manufacturer's instructions. Primer sequences and probes are given in **Supplementary table 4**. Relative induction of gene mRNA expression was calculated based on Ct values using the expression of *Hprt* for normalization. Data were expressed as fold change over controls.
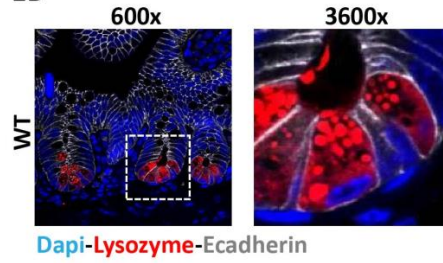
Statistical analysis

Data of 3–6 animals per experimental group are indicated. Statistical computations were performed using GraphPad Prism (GraphPad, La Jolla, CA). Statistical test used were: unpaired t-test for two group-comparisons or One-Way analysis of variances followed by Tukey test for comparisons comprising more than two groups. To determine statistically significant differences in *de novo* crypt formation, a Kruskal–Wallis test on ranks followed by Dunnś test was performed. Correlation analyses were performed according to Pearson test. Fisher-Exact test and Chi-Square test were performed to determine differences in the probability of recurrence of CD patients. Data are presented as mean ± standard error mean. and P-values bellow 0.05 were considered as statistically significant. Differences reached statistical significance with P values<0.05 (*), <0.01 (**) and P<0.001 (***).

Supplementary figures

1A

1B

600x   3600x

Dapi-**Lysozyme**-Ecadherin

1C

TNF^ΔARE

0   3.75

1200x   2400x

Lgr5- E-cadherin

1D

1E

1F

400x   1200x

WT

Lgr5

1G

TNF^ΔARE

0   2   5.75

400x   1200x

Olfm4

1H

r=- 0.9082
P<0.0001

1I

9
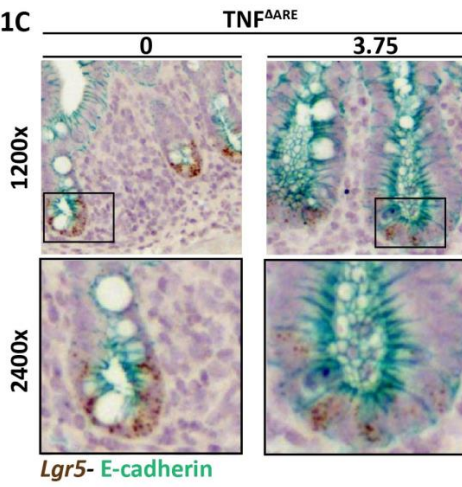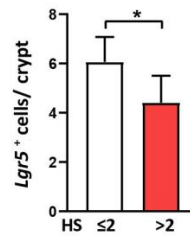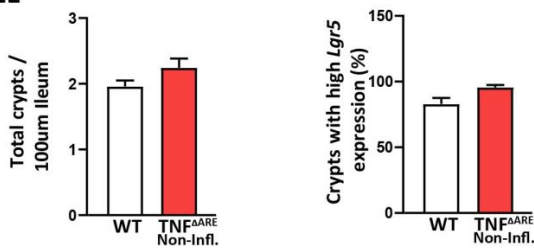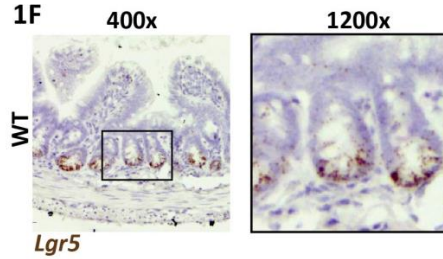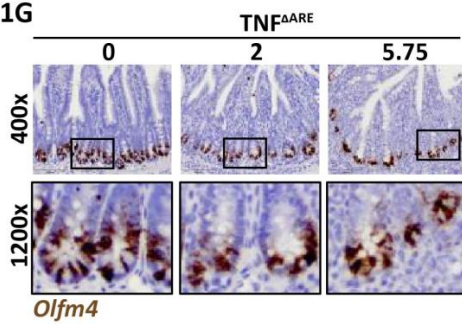
Supplementary figure 1: Inflammation but not genotype causes alterations in the ISC niche in TNF$^{\Delta ARE}$ mice

(**A, B**) Ileal tissue sections from non-inflamed TNF$^{\Delta ARE}$ and WT mice were analyzed. (**A**) Quantification of the total number of Lysozyme positive (Lyz$^+$) cells (left) and the proportion of highly granular Lyz$^+$ cells (≥2 granules). (**B**) Representative pictures of IF co-staining of Lysozyme (red) and E-cadherin (IEC borders, grey) counterstained with Dapi (nuclei, blue), including magnification showing Lyz$^+$ granules. (**C, D**) Ileal tissue sections from TNF$^{\Delta ARE}$ mice with different levels of inflammation were analyzed. (**C**) Representative pictures of *Lgr5 in situ* hybridization and IHC co-staining for E-cadherin. Numbers above indicate the respective histopathological score (HS). (**D**) Quantification of the number of *Lgr5$^+$* cells per crypt. (**E, F**) Ileal tissue sections from non-inflamed TNF$^{\Delta ARE}$ and WT mice were analyzed. (**E**) Quantification of the number of crypts (left) 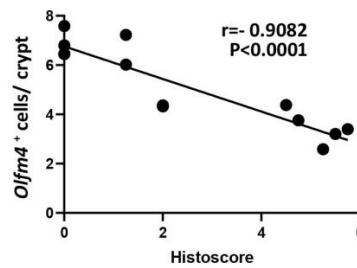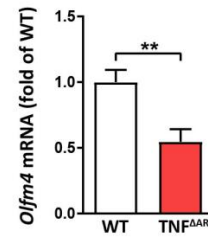and of *Lgr5 in situ* hybridization giving the proportion of crypts with high *Lgr5* expression (≥10 *Lgr5* transcripts). (**F**) Representative pictures of *Lgr5 in situ* hybridization in WT mice, including magnification. (**G, H**) Ileal tissue sections from TNF$^{\Delta ARE}$ mice with different levels of inflammation were analyzed. (**G**) Representative pictures of *Olfm4 in situ* hybridization, including magnifications; numbers indicate the respective histopathological score (HS). (**H**) Correlation analysis (Pearson) of the number of *Olfm4$^+$* cells and HS. (**I**) qRT-PCR analysis of TNF$^{\Delta ARE}$ and WT mice-derived IECs for *Olfm4* (N=5). Statistics were performed by unpaired *t*-test. Bars represent mean+s.e.m. Asterisks indicate significant differences *$P<0.05$, **$P<0.01$, ***$P<0.001$.
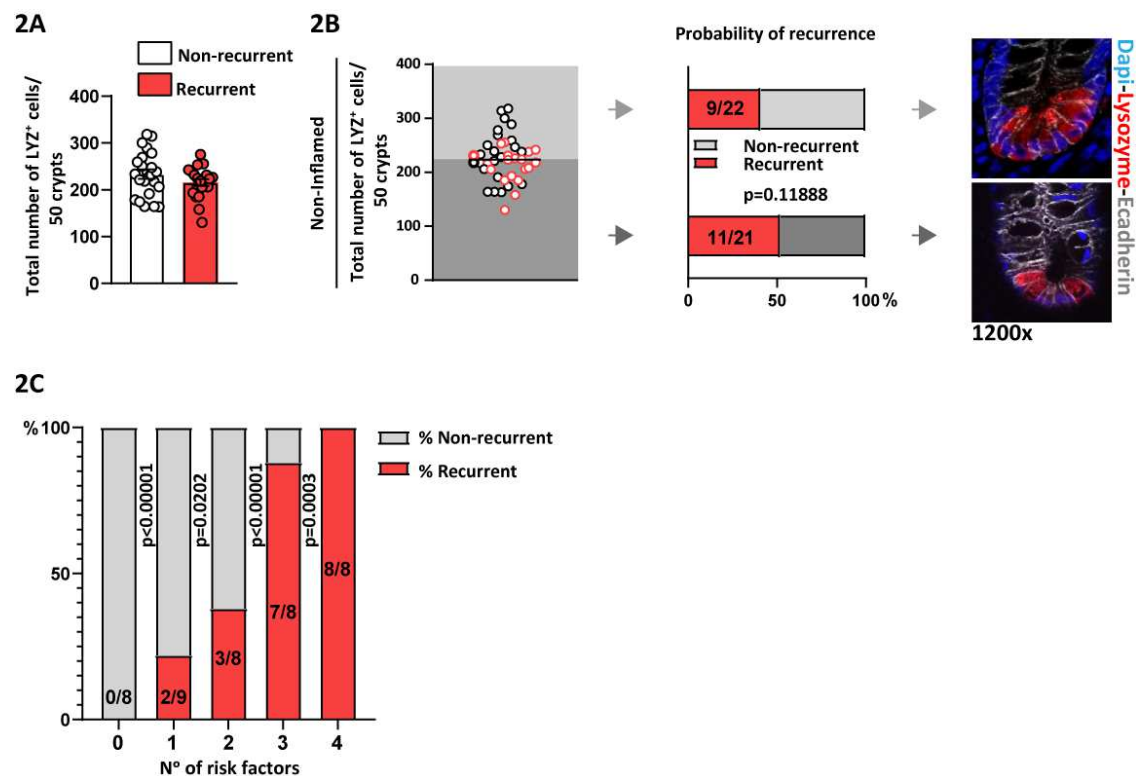
Supplementary figure 2: Risk of recurrence increases with the cumulative number of risk factors in CD patients non-inflamed at time of surgery

Ileal tissue sections classified as non-inflamed at time of surgery of CD patients undergoing resection surgery were analyzed. Tissue sections were stained for Lysozyme (LYZ) by IF and total number of LYZ positive cells in crypts were determined. CD patients with endoscopic recurrence (Rutgeerts score ≥i2) 6-12 months after surgery were compared to CD patients not experiencing recurrence. (**A**) overall comparison of recurrent versus non-recurrent patients for the total number of LYZ+ cells. Statistics were performed by unpaired *t*-test. Bars represent mean+s.e.m. (**B**) From left to right: distribution of the total number of LYZ+ cells among recurrent (red circles) and non-recurrent (black circles) CD patients with median indicated; probability of CD patients to experience recurrence if above or below the median for the respective marker; representative pictures showing sections from CD patients above or below median, IF co-staining of Lysozyme (red) and E-cadherin (IEC borders, grey) counterstained with Dapi (nuclei, blue). Chi-square test was used to determine significance. (**C**) Total numbers of highly granular PCs (below median), PCs in upper crypt (above median), highly *Lgr5* expressing crypts (below median) and *Lgr5* expression in upper crypts (above median) were assigned as risk factors resulting in a possible score from 0-4 for recurrent CD patients. The probability of CD patients non-inflamed at time of surgery to experience recurrence with indicated numbers of risk factors is shown. Statistical analyses were performed via Fisher-Exact test. Differences were considered statistically significant for *P*<0.05.
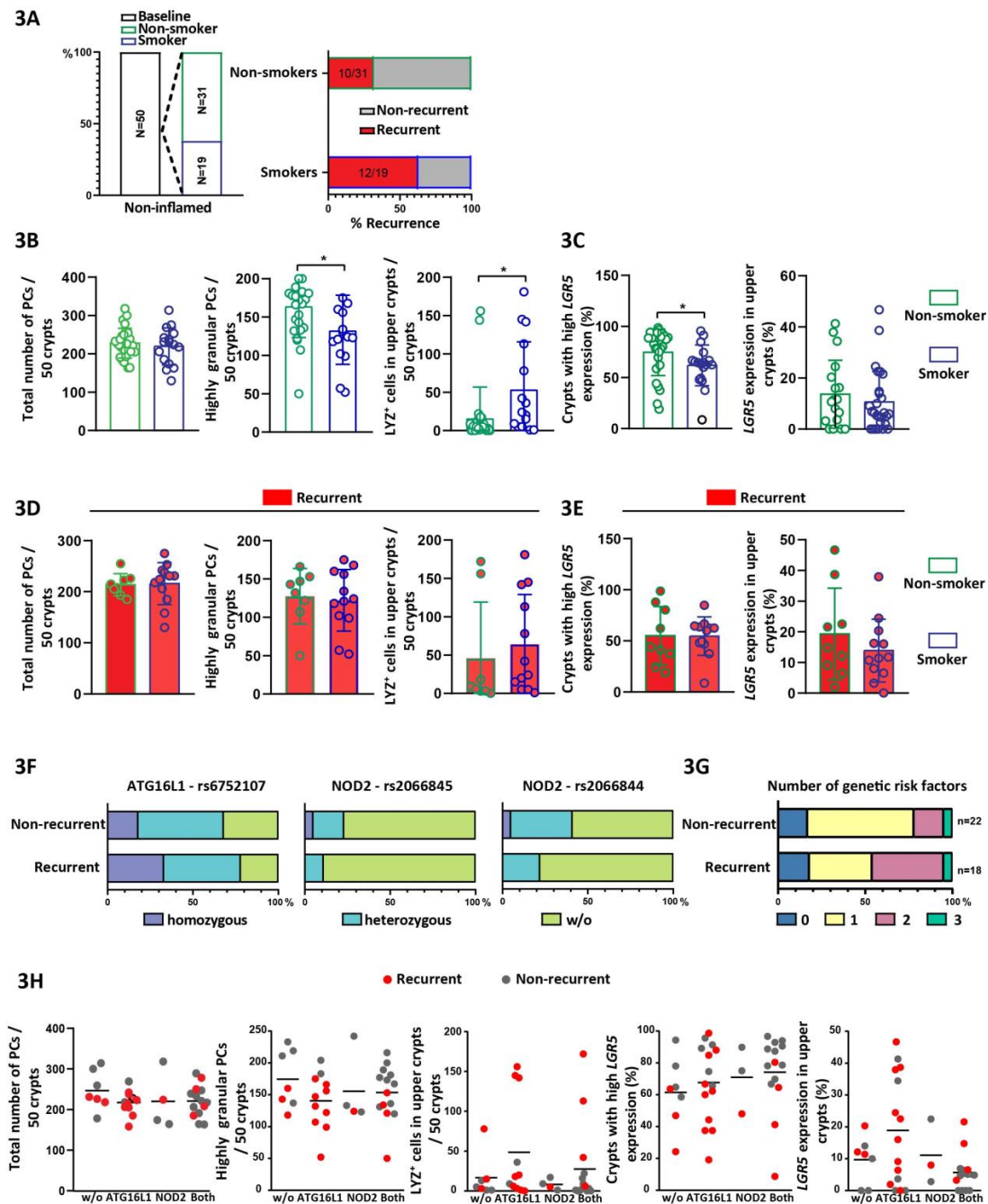
Supplementary figure 3: Smoking and genetic risk factors have no additional impact on ISC niche risk factors

Data from ileal tissue sections of CD patients undergoing resection surgery were analyzed for the smoking status of CD patients. (**A**) Overview of CD patient numbers and smoking status for baseline and endoscopic follow-up disease classification. (**B, C**) Total numbers of LYZ⁺ cells, numbers of highly granular LYZ⁺ cells (≥2 granules), numbers of LYZ⁺ cells in upper crypt, proportion of crypts with high *LGR5* expression (≥15 *LGR5* transcripts), and proportion of crypts with *LGR5* expression in upper crypt are depict for all patients regardless endoscopic follow-up disease classification according to the smoking. (**D, E**) The same readouts as in (**B**) and (**C**) are depict for patients experiencing endoscopic recurrence according to the smoking

12

status, showing no additional impact of smoking on the risk factors analyzed. (**F**) Distribution of CD-associated SNPs ATG16L1 rs6752107 and NOD2 rs2066845 or rs2066844 among recurrent and non-recurrent CD patients. (**G**) Numbers of risk alleles in recurrent and non-recurrent CD patients. (**H**) The same readouts as in (**B**) and (**C**) are depict according to patients´ genetics. Dots representing patients experiencing recurrence are given in red. No differences were found between genotypes for the risk factors analyzed. Statistical analyses were performed via unpaired *t*-test. Bars represent mean+s.e.m. Asterisks indicate significant differences *P<0.05.

4

Labelling	Inflamed	Probability of reccurence	Non-reccurrent vs Recurrent
Total number of LYZ+ cells / 50 crypts		6/8 (75%) / 4/7 (57%)	
Highly granular PCs / 50 crypts		7/9 (77%) / 3/6 (50%)	
LYZ+ cells in upper crypt/ 50 crypts		5/8 (63%) / 6/7 (86%)	
Crypts with high *LGR5* expression (%)		7/10 (70%) / 8/9 (88%)	
LGR5 expression in upper crypts (%)		7/10 (70%) / 8/9 (88%)	
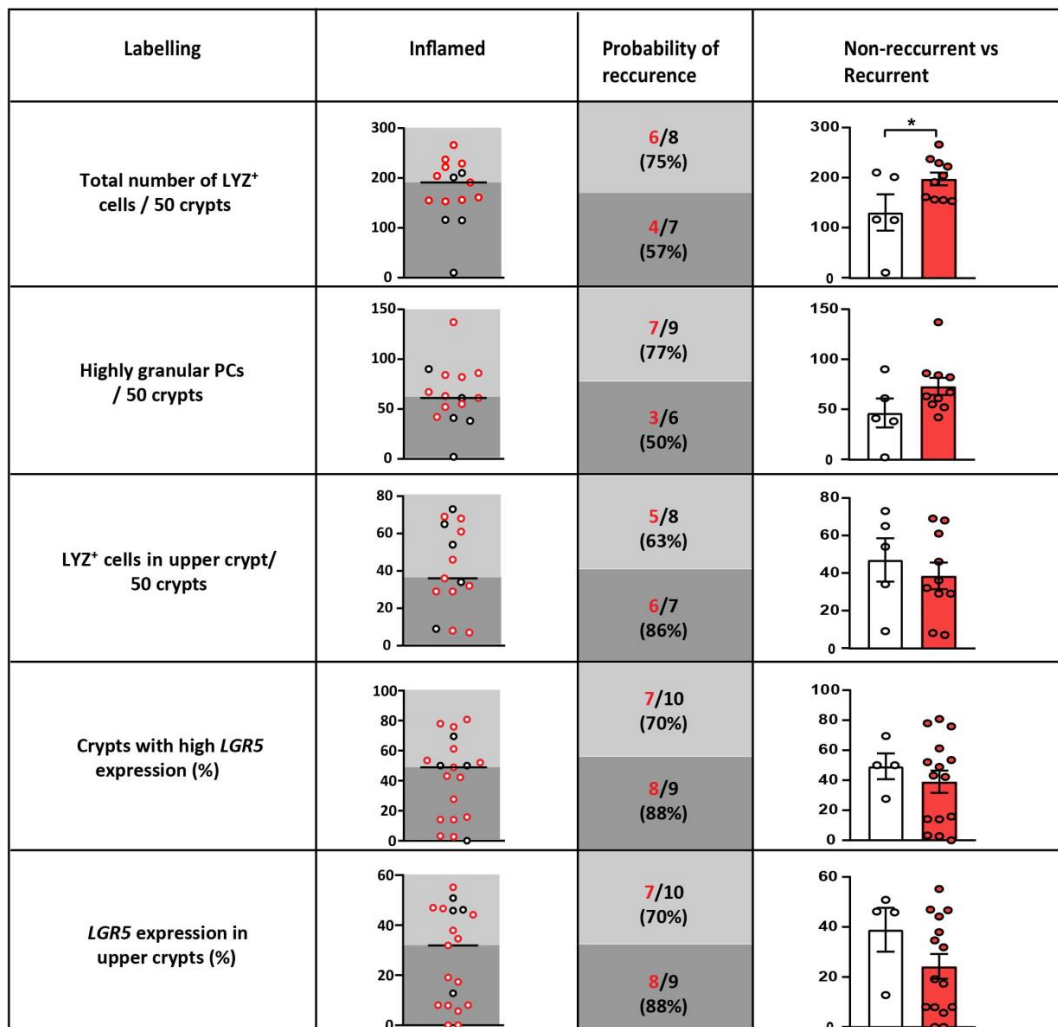
Supplementary figure 4: Paneth cell phenotype and *LGR5* expression pattern are not predictive for disease recurrence in inflamed CD patients

Ileal tissue sections classified as inflamed at time of surgery of CD patients undergoing resection surgery were analyzed. Tissue sections were stained for Lysozyme (LYZ) by IF and for *LGR5* by *in situ* hybridization, respectively, and expression patterns were quantified. From top to bottom: to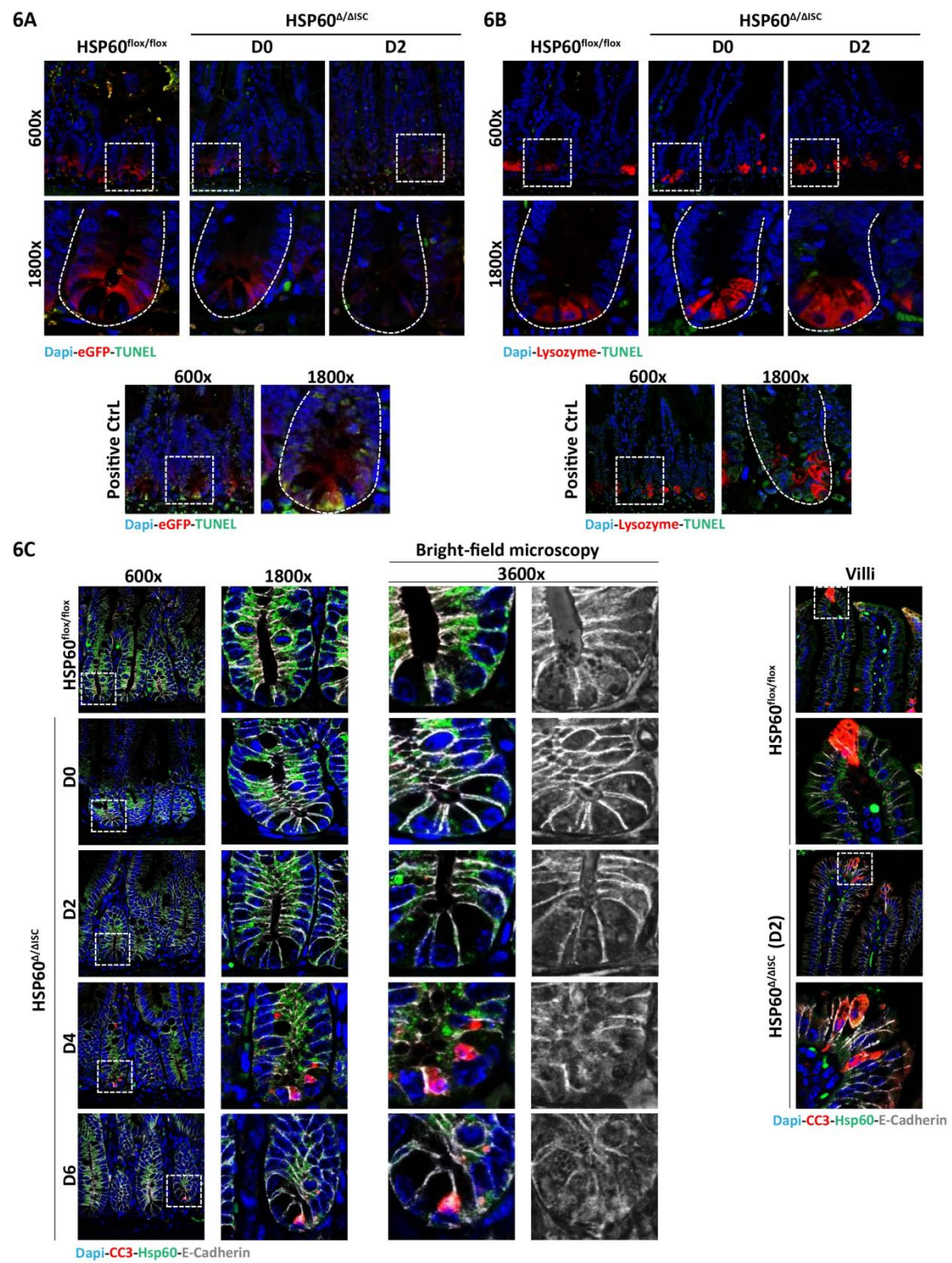tal numbers of LYZ+ cells, numbers of highly granular LYZ+ cells (≥2 granules), numbers of LYZ+ cells in upper crypt, proportion of crypts with high *LGR5* expression (≥15 *LGR5* transcripts), and proportion of crypts with *LGR5* expression in upper crypt were determined. CD patients with endoscopic recurrence (Rutgeerts score ≥i2) 6-12 months after surgery were compared to CD patients not experiencing recurrence. From left to right: distribution of the respective marker among recurrent (red circles) and non-recurrent (black circles) CD patients with median indicated; probability of CD patients to experience recurrence if above or below the median for the respective marker; overall comparison of recurrent versus non-recurrent patients for the respective marker. Statistics were performed by unpaired *t*-test. Bars represent mean+s.e.m. Asterisks indicate significant differences *P<0.05.

14
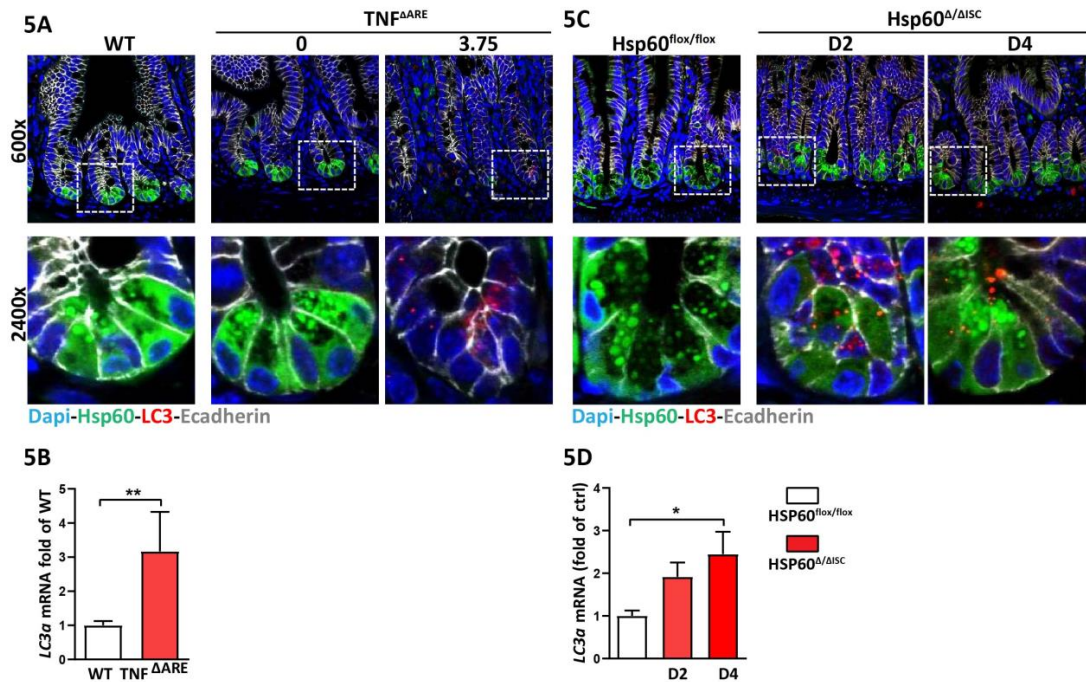
Supplementary figure 5: Induction of autophagy in mouse models of inflammation and mitochondrial dysfunction

Representative pictures of IF co-staining of LC3 (red), Hsp60 (green) and E-cadherin (IEC borders, grey) counterstained with Dapi (nuclei, blue) and qRT-PCR analysis of LC3a mRNA levels. (**A**) Ileal tissue sections from TNF$^{\Delta ARE}$ mice and WT littermates. Numbers above indicate the respective histopathological score (HS) (**B**) Primary isolated crypts from TNF$^{\Delta ARE}$ mice and WT littermates (N=5). (**C**) Ileal tissue sections from Hsp60$^{\Delta/\Delta ISC}$ and Hsp60$^{flox/flox}$ mice at D2 and D4 after end of tamoxifen treatment. (**D**) IEC isolates from Hsp60$^{\Delta/\Delta ISC}$ and Hsp60$^{flox/flox}$ mice. Statistical analysis was performed via unpaired *t*-test or One-way analysis of variance (ANOVA) followed by Tukey test when comparing more than two groups. Bars represent mean+s.e.m. Asterisks indicate significant differences *$P<0.05$, **$P<0.01$.

6A

Dapi-eGFP-TUNEL

6B

Dapi-Lysozyme-TUNEL

Dapi-eGFP-TUNEL

Dapi-Lysozyme-TUNEL

6C

Dapi-CC3-Hsp60-E-Cadherin

Dapi-CC3-Hsp60-E-Cadherin

16

Supplementary figure. 6: Loss of Hsp60 in intestinal stem cells induces apoptosis subsequently to loss of *Lgr5*-positive cells

Ileal tissue sections from Hsp60$^{\Delta/\Delta ISC}$ mice and Hsp60$^{flox/flox}$ controls were analyzed at different time points after end of tamoxifen treatment. (**A, B**) IF co-staining of eGFP (**A**, red, indicating *Lgr5* expressing cells) or lysozyme (Lyz) (**B**, red, indicating Paneth cells) and TUNEL staining (green, indicating apoptotic cells), for the indicated time-points, including magnifications. Lower panel: positive control for TUNEL assay (tissue sections treated with DNaseI), overlap of eGFP and TUNEL staining is indicated in yellow. (**C**) IF co-staining of cleaved caspase 3 (red, indicating apoptotic cells), Hsp60 (green) and E-cadherin (IEC borders, grey) counterstained with Dapi (nuclei, blue) in crypts; right side: magnifications including bright field images. Right panel: CC3 staining in villi, serving as a positive control.
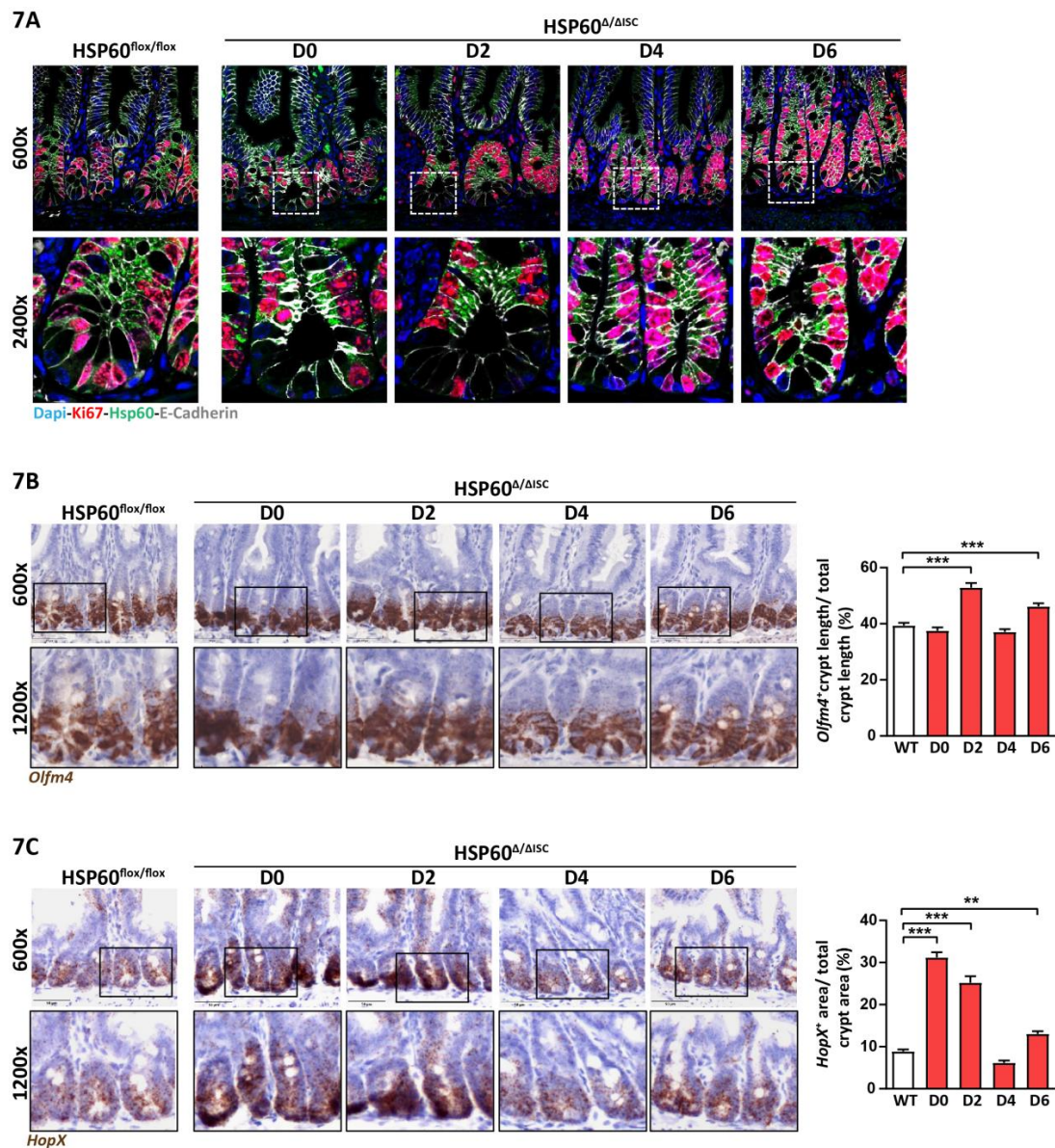
Supplementary figure 7: Hsp60 negative cells do not proliferate and remain in the crypt base, but crypts remain *Olfm4* and *Hopx* positive

Small intestinal tissue sections from Hsp60$^{\Delta/\Delta ISC}$ mice and Hsp60$^{flox/flox}$ controls were analyzed at different time points after end of tamoxifen treatment. (**A**) IF co-staining of Hsp60 (green), E-cadherin (IEC borders, grey) and Ki67 (proliferation, red) in ileal tissue sections. Dapi stains the nuclei in blue. (**B, C**) Left: representative pictures of *Olfm4* (**B**) and *Hopx* (**C**) *in situ* hybridization, including magnifications. (B) Right: quantification of the distance of the most upper *Olfm4* positive cell to the crypt ground normalized to crypt length (**C**) Right: quantification of the area positive for *Hopx* normalized to crypt area (N=3). Statistical analysis was performed via One-way analysis of variance (ANOVA) followed by Tukey test. Bars represent mean+s.e.m. Asterisks indicate significant differences *$P<0.05$, **$P<0.01$, ***$P<0.001$.

8A

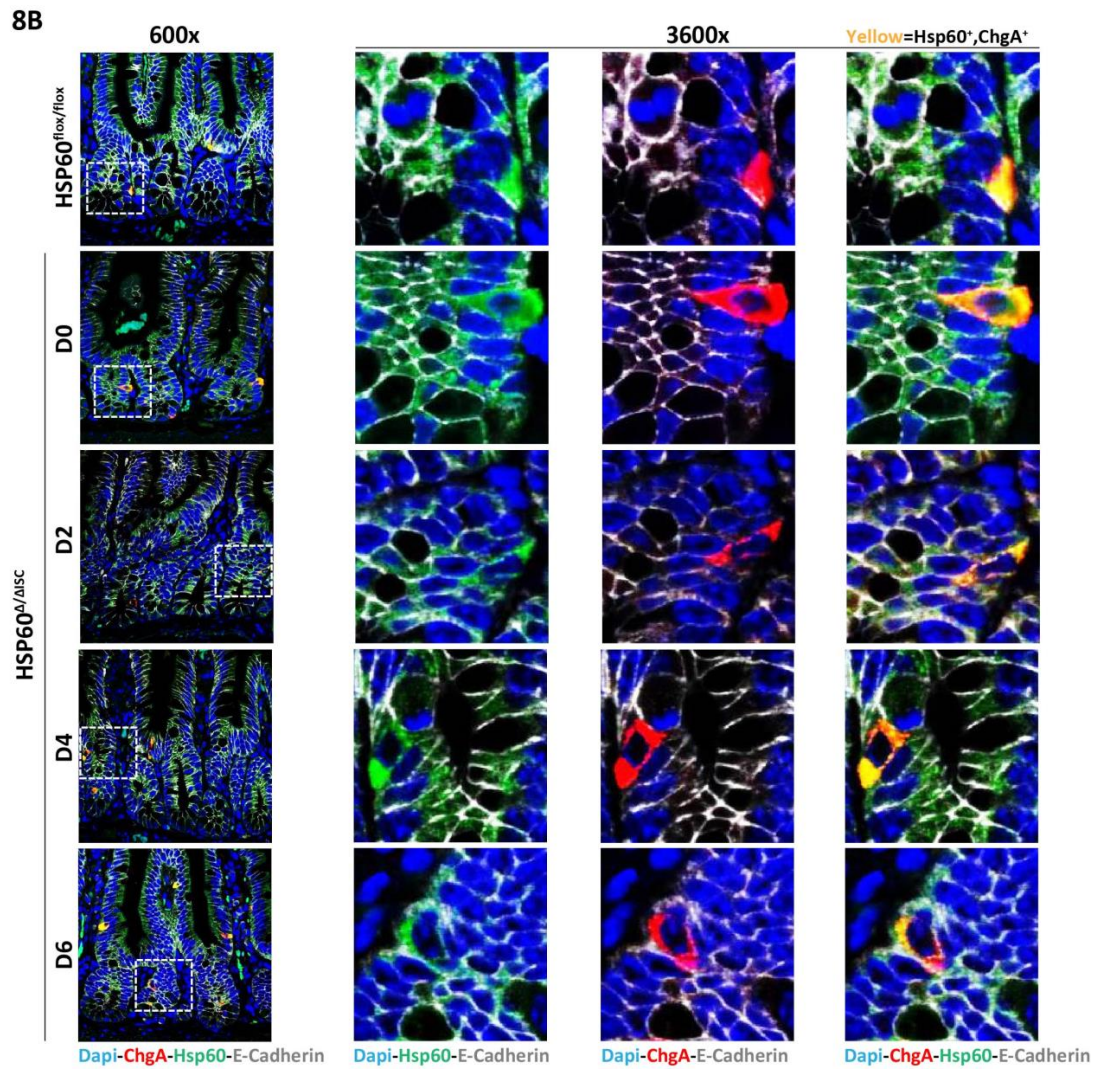Dapi-Muc2-Hsp60-E-Cadherin   Dapi-Hsp60-E-Cadherin   Dapi-Muc2-E-Cadherin   Dapi-Muc2-Hsp60-E-Cadherin

19

8B

600x | 3600x | Yellow=Hsp60⁺,ChgA⁺

HSP60^flox/flox

HSP60^Δ/ΔISC — D0, D2, D4, D6

Dapi-ChgA-Hsp60-E-Cadherin | Dapi-Hsp60-E-Cadherin | Dapi-ChgA-E-Cadherin | Dapi-ChgA-Hsp60-E-Cadherin

20
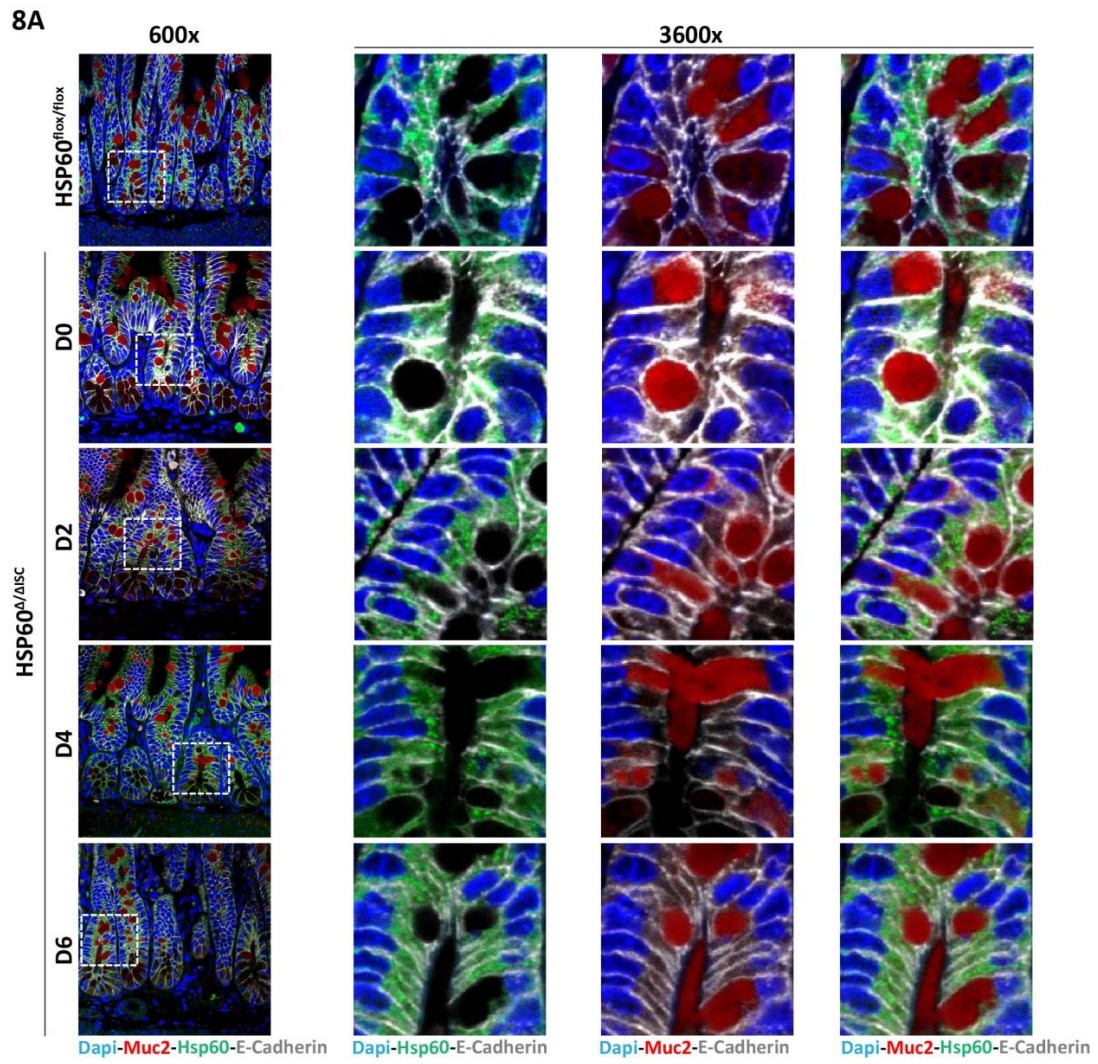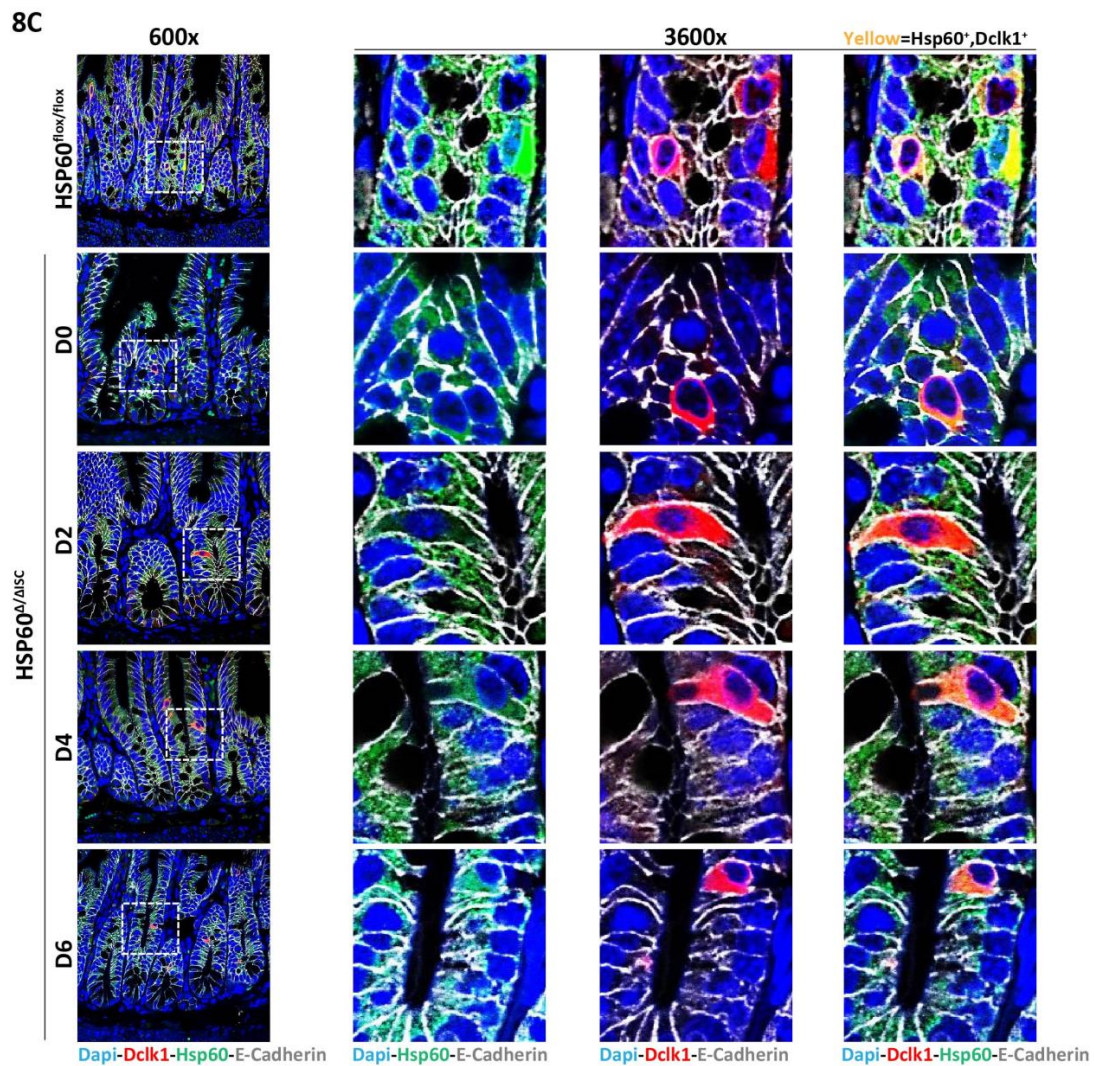
Supplementary figure 8: Hsp60 negative cells do not give rise to goblet cells, enteroendocrine cells or tuft cells

Ileal tissue sections from Hsp60$^{\Delta/\Delta ISC}$ mice and Hsp60$^{flox/flox}$ controls were analyzed at different time points after end of tamoxifen treatment. IF co-staining of Hsp60 (green), E-cadherin (IEC borders, grey) and (**A**) Muc2 (goblet cells, red), (**B**) ChgA (enteroendocrine cells, red), (**C**) Dclk1 (tuft cells) (red). Dapi stains the nuclei in blue. Muc2, ChgA and Cclk1 positive cell remain Hsp60 positive throughout the experiment.

21
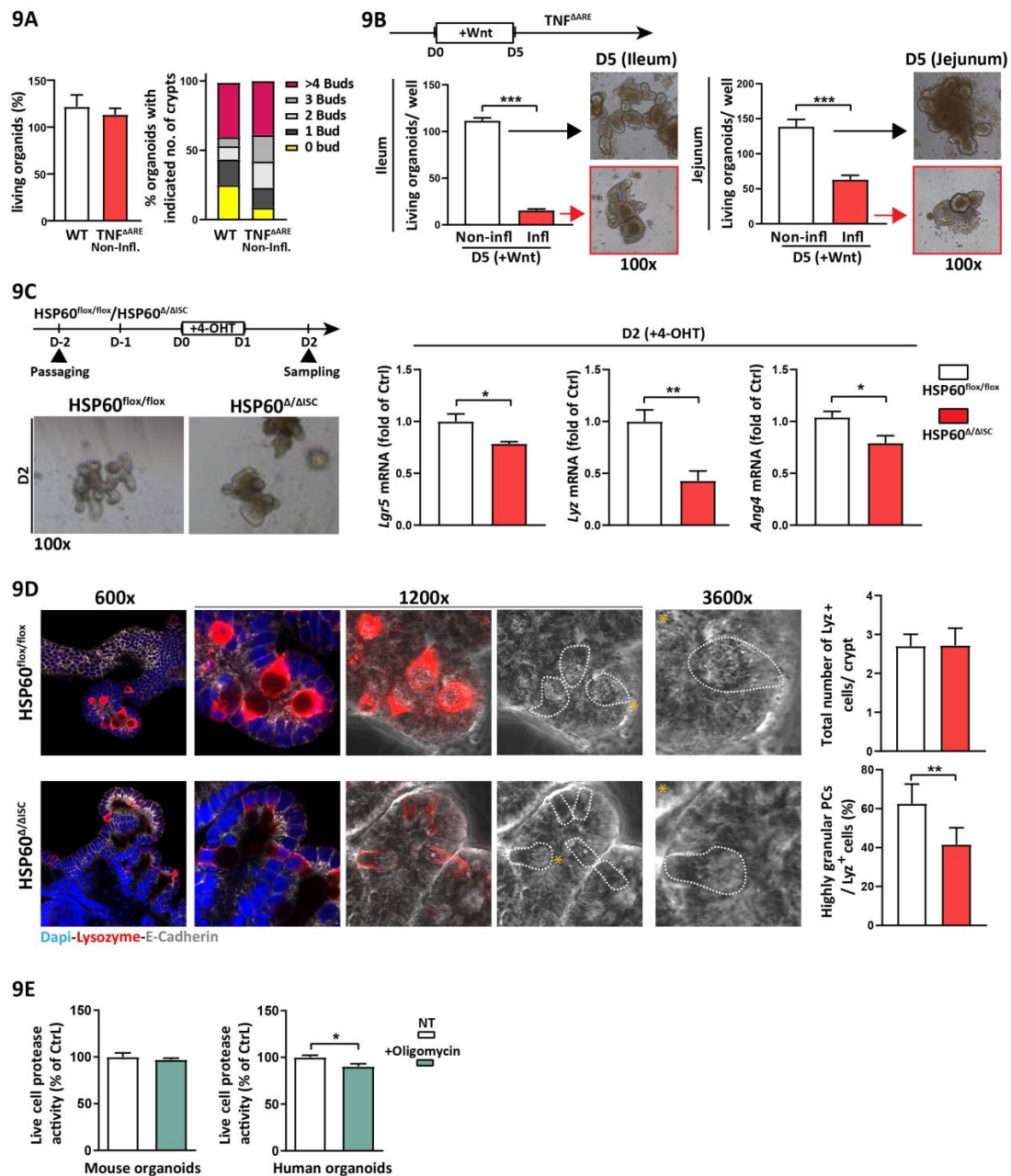
Supplementary figure 9: Wnt factor supplementation does not rescue growth of organoids derived from inflamed TNF$^{\Delta ARE}$ mice

(**A**) Growth characteristics of ileal organoids derived from non-inflamed TNF$^{\Delta ARE}$ mice and WT littermates. Left: proportion of living organoids; right: quantification of *de novo* crypt formation (budding) at day 5 of *ex vivo* culture. (**B**) Ileal (left) and jejunal (right) crypts derived from non-inflamed and inflamed TNF$^{\Delta ARE}$ mice were cultured in commercially available medium containing Wnt factors (Intesticult) for 5 days. Proportion of living organoids and representative bright field pictures are shown. (**C**) Organoids derived *Hsp60*$^{flox/flox}$ mice were treated with tamoxifen to induce ISC-specific Hsp60 loss and sampled 2 days later. Tamoxifen treated Cre negative organoids served as control. Left: representative bright field pictures; Right: qRT-PCR analysis of *Lgr5* and genes involved in PC function (N=6). (**D**) Representative pictures of IF

22

co-staining for Lysozyme (red) and E-cadherin (IEC borders, grey) counterstained with Dapi (nuclei, blue), including bright field pictures. Dotted lines indicate cell borders of Lyz positive (Lyz$^+$) cells; asterisks indicate Lyz$^+$ cells magnified in the pictures on the right side; Right: quantification of Lyz$^+$ cell numbers per crypt (upper graph) and the proportion of highly granular (≥2 granules) Lyz$^+$ cells (lower graph). (**E**) Measurement of living cells in murine (WT, left) and human (right) organoid cultures after treatment with oligomycin for 24h (N≥3). Statistical analysis was performed via unpaired *t*-test. Bars represent mean+s.e.m. Asterisks indicate significant differences *$P<0.05$, **$P<0.01$, ***$P<0.001$.
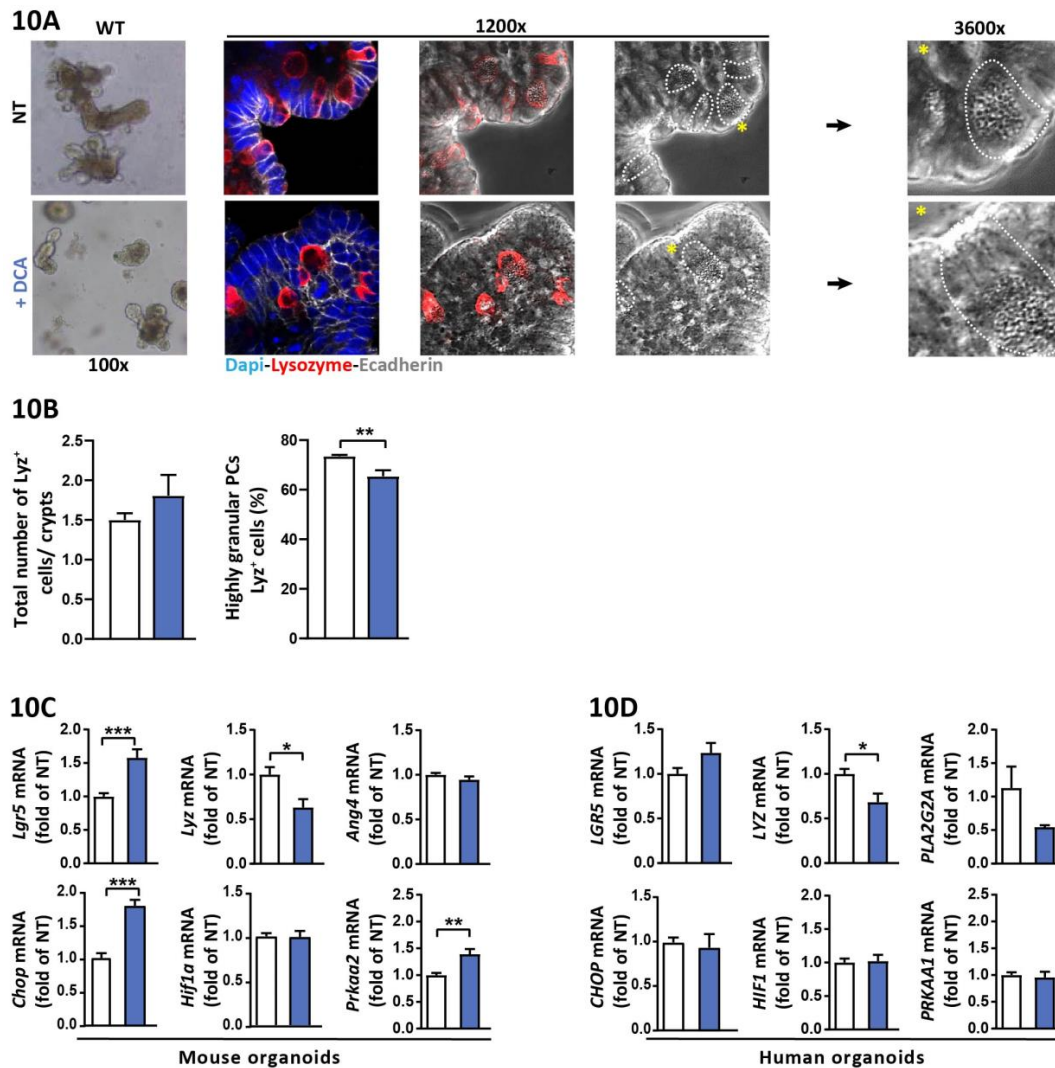
Supplementary figure 10: DCA treatment of WT ileal organoids
Ileal organoids derived from WT mice were treated with DCA for 24h. (**A**) Left: bright field and IF co-staining of Lyz (red) and E-cadherin (IEC borders, grey) counterstained with Dapi (nuclei, blue). Dotted lines indicate cell borders of Lyz positive (Lyz⁺) cells; asterisks indicate Lyz⁺ cells magnified in the pictures on the right side. (**B**) Quantification of Lyz⁺ cell numbers per crypt (left graph) and the proportion of highly granular (≥2 granules) Lyz⁺ cells (right graph). (**C**) qRT-PCR analysis of intestinal organoids for *Lgr5* and Paneth cell function-associated genes (upper panel) and for genes associated with mitochondrial signaling (lower panel, N=6). (**D**) Same analysis as in (**C**) for human organoids derived from the small intestine and treated with DCA for 24h (N=6). Statistical analysis was performed via unpaired *t*-test. Bars represent mean+s.e.m. Asterisks indicate significant differences *$P<0.05$, **$P<0.01$, ***$P<0.001$.

Supplementary tables

Table S1. **Patients' characteristics at time of surgery**.

Total number of patients included	n=70
Men	28 (40%)
Median age (y, IQR)	31.7 (26.4-44.0)
Age at Crohn's Disease diagnosis (Montreal classification)	
- ≤16 years (A1)	5 (7%)
- 17 - 40 years (A2)	56 (80%)
- >40 years (A3)	9 (13%)
Median disease duration (y, IQR)	6.7 (1.8-12.5)
Median time between resection and colonoscopy (mo, IQR)	6.7 (6.1-8.4)
Smoking	
- Active smoker	23 (33%)
- Smoking cessation at surgery	6 (9%)
- Non-smoker	41 (58%)
Previous intestinal resection	13 (19%)
Number of previous resection(s)	
– 0	57 (82%)
– 1	7 (10%)
– 2	3 (4%)
– 3	3 (4%)
Surgical indication	
– Stricturing complication	47 (67%)
– Penetrating complication	22 (31%)
– Failure of drug therapy	1 (2%)
Anoperineal lesion	13 (19%)
Extra-digestive symptoms	
- Joint manifestations	18 (26%)
- Skin manifestations	6 (9%)
- Eye manifestations	2 (3%)
Previous exposure to anti-TNF therapy	42 (60%)
Anti-TNF therapy within 3 months before surgery	29 (41%)
Previous exposure to thiopurines	53 (76%)
Thiopurines within 3 months before surgery	20 (29%)
Ileal resection margin inflamed	20 (29%)

Table S2. **Primary antibodies used in the study**.

Primary antibodies:	Species:	Company:	Dilution:
Anti-CC3	Rabbit	Cell signaling Technology, Danvers, MA	1:100
Anti-E-cadherin	Mouse	Abcam, Cambridge, UK	1:300
Anti-GFP (XP)	Rabbit	Cell signaling Technology, Danvers, MA	1:200
Anti-HSP60	Goat	Santa Cruz Biotechnology, Santa Cruz, CA	1:200
Anti-Lysozyme	Rabbit	Dako, Agilent, Santa Clara	1:1000
Anti-Chromogranin A	Rabbit	Abcam, Cambridge, UK	1:100
Anti-Dclk1	Rabbit	Biomol, Hamburg, Germany	1:100
Anti-Ki67	Rabbit	Cell signaling Technology, Danvers, MA	1:400
Anti-MAP LC3α/ß	Goat	Santa Cruz Biotechnology, Santa Cruz, CA	1:200
Anti-Muc2	Rabbit	BioTechne, Wiesbaden, Germany	1:200
Anti-PKR (M-515)	Rabbit	Santa Cruz Biotechnology, Santa Cruz, CA	1:100

Table S3. **Secondary antibodies used in the study**

Secondary antibodies:	Company:	Dilution:
HRP conjugated mouse anti goat IgG	Dianova, Hamburg, Germany	1:300
HRP conjugated donkey anti rabbit IgG	Dianova, Hamburg, Germany	1:300
Alexa Fluor donkey anti goat 488	Life Technologies, Carlsbad, CA	1:200
Alexa Fluor donkey anti rabbit 546	Life Technologies, Carlsbad, CA	1:200
Alexa Fluor donkey anti mouse 647	Life Technologies, Carlsbad, CA	1:200
Dapi	Sigma- Aldrich, Taufkirchen, Germany	1:1000

26

Table S4. **Primer sequences and probes for qRT-PCR**

Target genes Mouse:	Forward primer (L):	Reverse primer (R):	Probe:
Ang4	ccccagttggaggaaagc	cgtaggaatttttcgtacctttca	106
Atf5	tttttatgaagaggaataagatgaggt	ggaggctgcaccaacaat	16
Chop	cgacagagccagaataacagc	aagggttagacggagccagt	91
CoxIV	tcactgcgctcgttctgat	cgatcgaaagtatgagggatg	7
Defa5	ttttgggacctgcagaaatc	tggttgttgaccatccttgtt	84
Dll4	aggtgccacttcggttacac	gggagagcaaatggctgata	106
Grp78	ctgaggcgtatttgggaaag	tcatgacattcagtccagcaa	105
Hif1a	gcactagacaaagttcacctgaga	cgctatccacatcaaagcaa	95
Hprt	tcctcctcagaccgctttt	cctggttcatcatcgctaatc	95
Hsp10	ggcccgagttcagagtcc	tgtcaaagagcggaagaaactt	77
Hsp60	tcttcaggttgtggcagtca	cccctcttctccaaacactg	1
Lc3a	gaccagcaccccagtaagat	tgggaccagaaacttggtct	27
Lgr5	cttcactcggtgcagtgct	cagccagctaccaaataggtg	60
Lyz1	ggcaaaaccccaagatctaa	tctctcaccaccctctttgc	46
Olfm4	gaaattcgagagagagttttctaagg	gacctctactcggaccgtca	92
Otc	gctgtcatggtatccctgct	tttccttttgacaggcatca	99
Pdha	catcgttggagctcaggtg	cgccgtataatgtcaaacagac	15
Prkaa2	cagagcaaagcgtgtgacat	ttcttcttactcgaagatggtatgc	41
Trb3	gtcgctttgtcttcagcaact	tcatctgatccagtcatcacg	67
Yy1	ctggagaaaagccctttcag	gtcgaaggggcacacatag	94

Target genes Human:	Forward primer (L):	Reverse primer (R):	Probe:
CHOP	Cagagctggaacctgaggag	tgtttatggctgctttggtg	9
DLL1	gtggggagaaagtgtgcaa	tcacaaaatccatgctgctc	20
HIF1A	gaacctgatgctttaactttgct	tgctggtcatcagtttctgtg	28
HPRT1	tgatagatccattcctatgactgtaga	caagacattcttccagttaaagt	22
LGR5	accagactatgcctttggaaac	tcccagggagtggattctatt	78
LYZ	ccgctactggtgtaatgatgg	catcagcgatgttatcttgcag	68
PLA2G2A	aaatttctgagctacaagtttagcaac	ttatcacactcacacagttgacttct	32
PRKAA1	ctgatattttcatggtgatggaat	gacgccgactttcttttttca	63

References

1   Berger E, Rath E, Yuan D, Waldschmitt N, Khaloian S, Allgauer M, *et al.* Mitochondrial function controls intestinal epithelial stemness and proliferation. Nat Commun 2016;**7**:13171.

2   Harder U, Koletzko B, Peissner W. Quantification of 22 plasma amino acids combining derivatization and ion-pair LC-MS/MS. J Chromatogr B Analyt Technol Biomed Life Sci 2011;**879**:495-504.

3   Gucciardi A, Pirillo P, Di Gangi IM, Naturale M, Giordano G. A rapid UPLC-MS/MS method for simultaneous separation of 48 acylcarnitines in dried blood spots and plasma useful as a second-tier test for expanded newborn screening. Anal Bioanal Chem 2012;**404**:741-51.

4   Erben U, Loddenkemper C, Doerfel K, Spieckermann S, Haller D, Heimesaat MM, *et al.* A guide to histomorphological evaluation of intestinal inflammation in mouse models. Int J Clin Exp Pathol 2014;**7**:4557-76.

5   Auzolle C, Nancey S, Tran-Minh ML, Buisson A, Pariente B, Stefanescu C*, et al.* Male gender, active smoking and previous intestinal resection are risk factors for post-operative endoscopic recurrence in Crohn's disease: results from a prospective cohort study. Aliment Pharmacol Ther 2018;**48**:924-32.

6   Hammoudi N, Cazals-Hatem D, Auzolle C, Gardair C, Ngollo M, Bottois H*, et al.* Association Between Microscopic Lesions at Ileal Resection Margin and Recurrence After Surgery in Patients With Crohn's Disease. Clin Gastroenterol Hepatol 2019.

7   Zietek T, Rath E. Chapter 3 - Intestinal organoids: Mini-guts grown in the laboratory. In: Davies JA, Lawrence ML, eds. Organs and Organoids: Academic Press, 2018:43-71.